

SPIN

Modulations for quantum electronic material transports by vacuum annealing methods --Manuscript Draft--

Manuscript Number:	SPIN-D-23-00051R1
Full Title:	Modulations for quantum electronic material transports by vacuum annealing methods
Article Type:	Special Issue Paper
Keywords:	quantum electronic materials; vacuum annealing; magnetoresistance
Corresponding Author:	Ji-Wei Ci Chung Yuan Christian University TAIWAN
Corresponding Author Secondary Information:	
Corresponding Author's Institution:	Chung Yuan Christian University
Corresponding Author's Secondary Institution:	
First Author:	Ji-Wei Ci
First Author Secondary Information:	
Order of Authors:	Ji-Wei Ci Bo-Yu Chen Yuan-Chih Hung Huan-Chien Wang Dung-Sheng Tsai Wu-Yih Uen Yuan-Liang Zhong Jyh-Shyang Wang Chi-Te Liang Chiashain Chuang
Order of Authors Secondary Information:	
Abstract:	Gapless linear band structure quantum electronic materials play an important role in quantum computing developments due to their novel, superb electronic transport properties and two-dimensional gated device possibility. However, the sensitive surface of quantum electronic materials easily reacted with ambient air molecules so as to change their intrinsic transport properties. We review a series of our works to show the importance of surface reactions in quantum electronic materials, such as graphene. By using different electronic transport facilities and in-situ vacuum annealing methods, we are able to gently clean the absorbed air molecules on graphene so as to change the carrier densities and the electronic transport properties, which is a great improvement for 2D-quantum-material-based quantum chips and computing devices.
Response to Reviewers:	Response to Referee 1 Overall Comments from Reviewer #1: In the manuscript, the authors review a series of their works to show the importance of surface reactions in graphene. By removing the air molecules on graphene, the carrier densities and the electronic transport properties can be modified, which is beneficial for 2D-quantum-material-based chips and computing devices. Overall, this is a clear and well-organized manuscript; the topic of the manuscript also meets the requirement of SPIN. In my opinion, the manuscript is suitable for publication in SPIN after the authors have addressed the following questions and comments:

Question #1. On page 3, the authors mention that the adsorption of gases from the atmosphere can significantly affect the carrier density of single-layer graphene. Please explain more clearly how (increase or decrease) and why the carrier concentration of graphene is affected.

Our Reply #1. Thank you for your question about the effect of gas adsorption on the carrier density of single-layer graphene. We have addressed your concerns in the latest revision.

When gases from the atmosphere are adsorbed onto the graphene surface, they can lead to an alteration in the number of charge carriers (either electrons or holes) present in the material. This occurs due to the interaction between the adsorbed gas molecules and the graphene.

To comply with the Referee's comments,, we added the following sentences on page 2, paragraph 1 line 49-60:

"In the case of electron-donor gases, such as NH_3 , the adsorbed molecules can introduce additional electrons to the graphene structure. This results in an increase in the carrier concentration as the excess electrons contribute to the overall electron population available for conduction. Conversely, electron-acceptor gases, like oxygen (O_2), can lead to a decrease in the carrier density by effectively removing electrons from the graphene lattice. It's important to note that the specific effect of gas adsorption on carrier concentration depends on the type of gas, its affinity for graphene, and the interaction mechanism involved [11]."

Question #2. On page 3, the authors observed that the n-type graphene could be converted to p-type due to the absorption of water vapor and oxygen on the surface of epitaxial graphene. Although P-type graphene can be realized through both oxygen and water vapor, water vapor and oxygen have different effects on graphene in terms of longitudinal magnetoresistance (Fig. 3a) and Hall resistance (Fig. 3b). Why? Please explain the reasons in detail so that readers can more easily understand the properties of graphene.

Our reply #2. Thank you for your inquiry regarding the differences in the effects of water vapor and oxygen. We have elaborated the reasons in detail in our latest revision.

In accordance with the Referee's comments, we have added the following sentences on page 3, paragraph 1, line 18-34:

"Notably, the more pronounced effect induced by water vapor, as compared to oxygen, on the property of graphene can be attributed to the specific interaction mechanisms between these two gases and the graphene lattice. In the case of water vapor, it interacts with the graphene surface through adsorption and dissociation processes. When water vapor molecules are adsorbed onto the graphene, they dissociate into hydrogen (H) and hydroxyl (OH) radicals. The introduction of hydrogen and hydroxyl groups can alter the charge carrier concentration in the graphene layer. The hydrogen atoms can effectively change the doping level and contribute to the observed dR_{xy}/dB slope change in electrical behavior due to Hall effect, leading to changes in longitudinal magnetoresistance and Hall resistance [11]."

Question #3. In Fig. 5, the chamber temperature can be reduced to 4.6 K. Why are you measuring the properties of graphene in a 6 K environment?

Our reply #3. Thank you for pointing this out. 4.6 K is the temperature that our system can reach without sample and any treatments. Since the measurement involves providing current for the graphene sample, the heating effect of current increases the temperature of the system. Therefore, the measurement is more suitable to conduct at the temperature higher than 4.6 K.

To comply with the Referee's comments, we have corrected the following sentence on

page 4, paragraph 1, line 9-12:

"As shown in Fig. 6, in our measuring system we firstly decreased the sample temperature to 6 K as a stable measuring temperature to measure magnetoresistance under $P = 10^{-3}$ Torr before vacuum annealing."

Question #4. On page 4, Why nickel- catalyzed graphene has fewer defects and charged impurities than copper-catalyzed graphene. Please explain the reasons in detail so that readers can understand graphene deeply.

Our reply #4. Thank you for your inquiry regarding the discrepancy in defect and charged impurity levels between nickel-catalyzed and copper-catalyzed graphene. Nickel and copper have distinct reactivity with carbon atoms during the catalytic growth process.

In accordance with the Referee's comments, we added the following sentences on page 3, paragraph 1, line 39-47:

"Remarkably, nickel forms a stronger interaction with carbon due to the releasing carbon atoms to the nickel surface from nickel films, leading to a more controlled growth mechanism [18]. This results in fewer defects introduced during the initial stages of graphene formation. Copper, on the other hand, tends to exhibit a weaker interaction due to the carbon absorption on the copper surface, potentially leading to more defects and impurities [19]."

Also, we have added two references (Refs. 18 and 19).

18. A. Reina, X. Jia, J. Ho, D. Nezich, H. Son, V. Bulovic, M. S. Dresselhaus, J. Kong, Nano Lett. 9, 30 (2009).

19. X. Li, W. Cai, J. An, S. Kim, J. Nah, D. Yang, R. Piner, A. Velamakanni, I. Jung, E. Tutuc, S. K. Banerjee, L. Colombo, R. S. Ruoff, Science 324, 1312 (2009).

Response to Referee 2

Overall Comment from Reviewer #2: The authors can keep the epitaxial graphene Hall device in the vacuum chamber above the closed gate valve and inject various gases into the chamber overnight, allowing the graphene surface to absorb the gas. The leftover gas can then be pumped out, and the gate valve can be opened to insert the epitaxial Hall gadget into the sample area with a superconducting magnet for low-temperature magnetoresistance measurements. This work is interesting and meaningful, but the manuscript format may need minor adjustments before publication.

Question #1. Some text or numbers in the figure are too small to see; please fix it. For example, in Fig. 1, NH_3 , CO , etc. are really too small to see, even to notice. We acknowledge that the original labels and numbers in the figure were unclear. We have made necessary modifications in the latest revision.

Our reply #1. We acknowledge that the original wording and numbers in the figure was unclear. However, the raw data in literature is unavailable. We have made necessary modifications for Fig. 1 in the latest revision.

Question #2. All numbers and text format in figures are inconsistent; please fix it.

Our reply #2. We appreciate your attention. However, due to the unavailability of raw data in the literature, we have made our best efforts to address the inconsistency. Specifically, we have adjusted the size of the temperature label in Figure 6 to ensure uniformity.

Question #3. It is fascinating to compare the magnetic property difference between copper-catalyzed graphene and nickel-catalyzed graphene; but in Fig. 6, a, b, and c measurements were done at 6 K, but Fig. 6 d was measured at 15K but not 6 K. Is

there any specific reason for the magnetoresistance of nickel- and copper-catalyzed graphene at T = 15 K after vacuum annealing?

Our reply #3. We appreciate your observation. In Fig. 6(c), the relative magnetoresistance (%) before and after vacuum annealing at low temperatures of 6 K is derived from the data presented in Fig. 6(a) and Fig. 6(b). To clarify, we have included the mathematical formulation for relative magnetoresistance in the revised version. The decision to present the MR values for nickel- and copper-catalyzed graphene at T = 15 K as Fig. 6(d) is to emphasize the obvious changes before and after vacuum annealing although we particularly raised up the measuring temperature to 15 K, which is highlight the consistency of magnetoresistance across different temperatures.

To comply with the Referee's comments,, we added the following sentence on page 3, paragraph 1, line 28-31:

"Here the relative magnetoresistance is given by $MR_{relative} = [R_{after}(B) - R_{before}(B)] / R_{before}(B) \times (100\%)$, where $R_{after}(B)$ and $R_{before}(B)$ are the resistances at certain magnetic field before and after vacuum annealing, respectively."

Also, we updated the caption of Fig. 6 :

"Fig. 6. Comparison of the magnetoresistance transport properties of nickel and copper-catalyzed graphene before and after vacuum annealing (a) the magnetoresistance of nickel-catalyzed graphene at T = 6 K before and after vacuum annealing (b) the magnetoresistance of copper-catalyzed graphene at T = 6 K before and after vacuum annealing (c) the relative magnetoresistance of nickel and copper-catalyzed graphene at T = 6 K after vacuum annealing in comparison with before vacuum annealing (d) the relative magnetoresistance of nickel and copper-catalyzed graphene at T = 15 K after vacuum annealing [17]."

Dear Editor,

Thank you for sending us the Referees' reports on our manuscript SPIN-D-23-00051 by Ji-Wei Ci *et al.* We thank the Referees for their insightful questions and reviews. We have answered all the questions and addressed all the problems in detail in the latest revision. All the changes or modifications made from the submitted version are highlighted in this updated draft. In addition, please note that the second author Bo-Yu Chen adds "Department of Physics at National Taiwan University" as his affiliation, since he just became a freshman in that affiliation. These revisions include additional explanations and modified graphs to help readers build background knowledge and visual demonstrations of properties of graphene. We acknowledge that the suggestion from Referee 1 for revisions to enhance clarity and readability should be incorporated before accepting the manuscript for publication. Furthermore, Referee 2 also supports considering the manuscript for publication after minor adjustments. Therefore, we hope that our revised manuscript is now suitable for publication in SPIN.

Sincerely

Associate Prof. Chiashain Chuang
Chung Yuan Christian University
Taiwan

Response to Referees

Response to Referee 1

Overall Comments from Reviewer #1: In the manuscript, the authors review a series of their works to show the importance of surface reactions in graphene. By removing the air molecules on graphene, the carrier densities and the electronic transport properties can be modified, which is beneficial for 2D-quantum-material-based chips and computing devices. Overall, this is a clear and well-organized manuscript; the topic of the manuscript also meets the requirement of SPIN. In my opinion, the manuscript is suitable for publication in SPIN after the authors have addressed the following questions and comments:

Question #1. On page 3, the authors mention that the adsorption of gases from the atmosphere can significantly affect the carrier density of single-layer graphene. Please explain more clearly how (increase or decrease) and why the carrier concentration of graphene is affected.

Our Reply #1. Thank you for your question about the effect of gas adsorption on the carrier density of single-layer graphene. We have addressed your concerns in the latest revision.

When gases from the atmosphere are adsorbed onto the graphene surface, they can lead to an alteration in the number of charge carriers (either electrons or holes) present in the material. This occurs due to the interaction between the adsorbed gas molecules and the graphene.

To comply with the Referee's comments,, we added the following sentences on page 2, paragraph 1 line 49-60:

“In the case of electron-donor gases, such as NH_3 , the adsorbed molecules can introduce additional electrons to the graphene structure. This results in an increase in the carrier concentration as the excess electrons contribute to the overall electron population available for conduction. Conversely, electron-acceptor gases, like oxygen (O_2), can lead to a decrease in the carrier density by effectively removing electrons from the graphene lattice. It's important to note that the specific effect of gas adsorption on carrier concentration depends on the type of gas, its affinity for graphene, and the interaction mechanism involved [11].”

Question #2. On page 3, the authors observed that the n-type graphene could be converted to p-type due to the absorption of water vapor and oxygen on the surface of epitaxial graphene. Although P-type graphene can be realized through both oxygen and water vapor, water vapor and oxygen have different effects on graphene in terms of longitudinal magnetoresistance (Fig. 3a) and Hall resistance (Fig. 3b). Why? Please explain the reasons in detail so that readers can more easily understand the properties of graphene.

Our reply #2. Thank you for your inquiry regarding the differences in the effects of water vapor and oxygen. We have elaborated the reasons in detail in our latest revision.

In accordance with the Referee's comments, we have added the following sentences on page 3, paragraph 1, line 18-34:

“Notably, the more pronounced effect induced by water vapor, as compared to oxygen, on the property of graphene can be attributed to the specific interaction mechanisms between these two gases and the graphene lattice. In the case of water vapor, it interacts with the graphene surface through adsorption and dissociation processes. When water vapor molecules are adsorbed onto the graphene, they dissociate into hydrogen (H) and hydroxyl (OH) radicals. The introduction of hydrogen and hydroxyl groups can alter the charge carrier concentration in the graphene layer. The hydrogen atoms can effectively change the doping level and contribute to the observed dR_{xy}/dB slope change in electrical behavior due to Hall effect, leading to changes in longitudinal magnetoresistance and Hall resistance [11].”

Question #3. In Fig. 5, the chamber temperature can be reduced to 4.6 K. Why are you measuring the properties of graphene in a 6 K environment?

Our reply #3. Thank you for pointing this out. 4.6 K is the temperature that our system can reach without sample and any treatments. Since the measurement involves providing current for the graphene sample, the heating effect of current increases the temperature of the system. Therefore, the measurement is more suitable to conduct at the temperature higher than 4.6 K.

To comply with the Referee's comments, we have corrected the following sentence on page 4, paragraph 1, line 9-12:

“As shown in Fig. 6, in our measuring system we firstly decreased the sample temperature to 6 K as a stable measuring temperature to measure magnetoresistance under $P = 10^{-3}$ Torr before vacuum annealing.”

Question #4. On page 4, Why nickel-catalyzed graphene has fewer defects and charged impurities than copper-catalyzed graphene. Please explain the reasons in detail so that readers can understand graphene deeply.

Our reply #4. Thank you for your inquiry regarding the discrepancy in defect and charged impurity levels between nickel-catalyzed and copper-catalyzed graphene. Nickel and copper have distinct reactivity with carbon atoms during the catalytic growth process.

In accordance with the Referee's comments, we added the following sentences on page 3, paragraph 1, line 39-47:

“Remarkably, nickel forms a stronger interaction with carbon due to the releasing carbon atoms to the nickel surface from nickel films, leading to a more controlled growth mechanism [18]. This results in fewer defects introduced during the initial stages of graphene formation. Copper, on the other hand, tends to exhibit a weaker interaction due to the carbon absorption on the copper surface, potentially leading to more defects and impurities [19].”

Also, we have added two references (Refs. 18 and 19).

18. A. Reina, X. Jia, J. Ho, D. Nezich, H. Son, V. Bulovic, M. S. Dresselhaus, J. Kong, *Nano Lett.* 9, 30 (2009).

19. X. Li, W. Cai, J. An, S. Kim, J. Nah, D. Yang, R. Piner, A. Velamakanni, I. Jung, E. Tutuc, S. K. Banerjee, L. Colombo, R. S. Ruoff, *Science* 324, 1312 (2009).

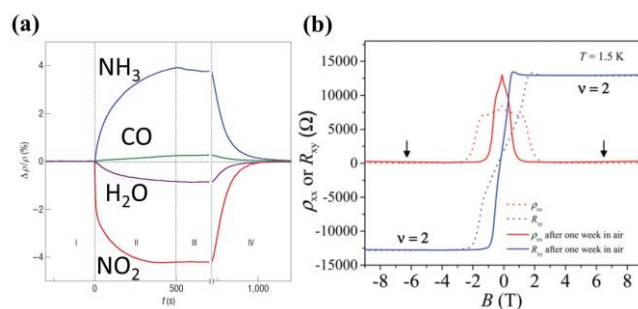
Response to Referee 2

Overall Comment from Reviewer #2: The authors can keep the epitaxial graphene Hall device in the vacuum chamber above the closed gate valve and inject various gases into the chamber overnight, allowing the graphene surface to absorb the gas. The leftover gas can then be pumped out, and the gate valve can be opened to insert the epitaxial Hall gadget into the sample area with a superconducting magnet for low-temperature magnetoresistance measurements. This work is interesting and meaningful, but the manuscript format may need minor adjustments before publication.

Question #1. Some text or numbers in the figure are too small to see; please fix it. For example, in Fig. 1, NH₃, CO, etc. are really too small to see, even to notice.

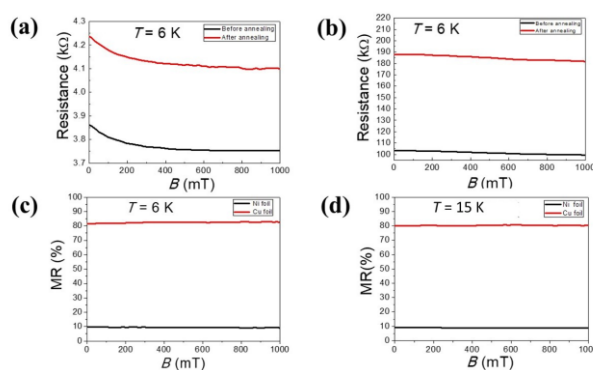
We acknowledge that the original labels and numbers in the figure were unclear. We have made necessary modifications in the latest revision.

Our reply #1. We acknowledge that the original wording and numbers in the figure was unclear. However, the raw data in literature is unavailable. We have made necessary modifications for Fig. 1 in the latest revision.



Question #2. All numbers and text format in figures are inconsistent; please fix it.

Our reply #2. We appreciate your attention. However, due to the unavailability of raw data in the literature, we have made our best efforts to address the inconsistency. Specifically, we have adjusted the size of the temperature label in Figure 6 to ensure uniformity.



Question #3. It is fascinating to compare the magnetic property difference between

copper-catalyzed graphene and nickel-catalyzed graphene; but in Fig. 6, a, b, and c measurements were done at 6 K, but Fig. 6 d was measured at 15K but not 6 K. Is there any specific reason for the magnetoresistance of nickel- and copper-catalyzed graphene at $T = 15$ K after vacuum annealing?

Our reply #3. We appreciate your observation. In Fig. 6(c), the relative magnetoresistance (%) before and after vacuum annealing at low temperatures of 6 K is derived from the data presented in Fig. 6(a) and Fig. 6(b). To clarify, we have included the mathematical formulation for relative magnetoresistance in the revised version. The decision to present the MR values for nickel- and copper-catalyzed graphene at $T = 15$ K as Fig. 6(d) is to emphasize the obvious changes before and after vacuum annealing although we particularly raised up the measuring temperature to 15 K, which is highlight the consistency of magnetoresistance across different temperatures.

To comply with the Referee's comments,, we added the following sentence on page 3, paragraph 1, line 28-31:

“Here the relative magnetoresistance is given by $MR_{\text{relative}} = [R_{\text{after}}(B) - R_{\text{before}}(B)]/R_{\text{before}}(B) \times (100\%)$, where $R_{\text{after}}(B)$ and $R_{\text{before}}(B)$ are the resistances at certain magnetic field before and after vacuum annelaing, respecitvely.”

Also, we updated the caption of Fig. 6 :

“Fig. 6. Comparison of the magnetoresistance transport properties of nickel and copper-catalyzed graphene before and after vacuum annealing (a) the magnetoresistance of nickel-catalyzed graphene at $T = 6$ K before and after vacuum annealing (b) the magnetoresistance of copper-catalyzed graphene at $T = 6$ K before and after vacuum annealing (c) the relative magnetoresistance of nickel and copper-catalyzed graphene at $T = 6$ K after vacuum annealing in comparison with before vacuum annealing (d) the relative magnetoresistance of nickel and copper-catalyzed graphene at $T = 15$ K after vacuum annealing [17].”

SPIN
Vol. 1, No. 1 (2011) 1–4
©World Scientific Publishing Company

Modulations for quantum electronic material transports by vacuum annealing methods

JI-WEI CI

Department of Electronic Engineering

*Chung Yuan Christian University
Taoyuan 320, Taiwan*

BO-YU CHEN

Department of PHYSICS

*National Taiwan University
Taipei 106, Taiwan*

Department of Electronic Engineering

*Chung Yuan Christian University
Taoyuan 320, Taiwan*

YUAN-CHIH HUNG, HUAN-CHIEN WANG, DUNG-SHENG TSAI and WU-YIH UEN

Department of Electronic Engineering

*Chung Yuan Christian University
Taoyuan 320, Taiwan*

YUAN-LIANG ZHONG and JYH-SHYANG WANG

Department of PHYSICS

*Chung Yuan Christian University
Taoyuan 320, Taiwan*

CHI-TE LIANG

Department of PHYSICS

*National Taiwan University
Taipei 106, Taiwan*

CHIASHAIN CHUANG*

*Department of Electronic Engineering**Chung Yuan Christian University
Taoyuan 320, Taiwan**Research Center for Semiconductor Materials and Advanced Optics**Chung Yuan Christian University
Taoyuan 320, Taiwan**chiashain@cycu.edu.tw*

Gapless linear band structure quantum electronic materials play important roles in quantum computing developments due to their novel superb electronic transport properties and two-dimensional gateable device possibility. However, the sensitive surface of quantum electronic materials easily reacted with ambient air molecules so as to change their intrinsic transport properties. We review a series of our works to show the importance of surface reactions in quantum electronic materials, such as graphene. By using different electronic transport facilities and in-situ vacuum annealing methods, we are able to gently clean the absorbed air molecules on graphene so as to change the carrier densities and the electronic transport properties, which is a great improvement for 2D-quantum-material-based quantum chips and computing devices.

Keywords: quantum electronic materials, vacuum annealing, magnetoresistance.

1. Introduction

Since the first time to exfoliate single-layer graphene by using Scotch tape by Novoselov and Geim in 2004 [1], several novel atomic layer quantum electronic materials have been extensively studied. These materials include MoS₂ with suitable bandgap [2], black phosphorus with a narrow bandgap [3], h-BN with a hexagonal crystal structure and wide bandgap [4], SnSe₂ with thermoelectric and optoelectronic properties [5-7], the topological Dirac semimetal Cd₃As₂ [8], the Weyl semimetal MoTe₂ [9], the two-dimensional (2D) magnetic material VS₂ [10] and so on. As the aforementioned quantum electronic materials are ultrathin to only a few atomic layers, their surfaces are extremely sensitive to gases in the atmosphere. Some molecular gases absorbed on the material surface often lead to significant changes in their physical and chemical properties.

For instance, Novoselov and Geim found that single-layer graphene significantly altered its conductivity while exposing to different gases (NO₂, H₂O, CO and NH₃) so as to change the carrier property to either n-type or p-type semimetal, as shown in Fig. 1 (a). Therefore, single-layer graphene can be applied to

gas sensors and related applications [11]. On the other hand, it was found that the longitudinal and transverse Hall resistances are significantly affected by the adsorption of gases in the atmosphere when the single-layer epitaxial graphene was made into a quantum Hall device as a resistance standard performance, which affected the resistance accuracy of the quantum Hall magnetoresistance plateau ($\nu = 2$) as shown in Fig. 1(b) [12]. The sensitive surface effects of quantum electronic materials mostly stem from their large surface area to volume ratio. Therefore, tuning the annealing temperature and time in vacuum conditions to enhance gas desorption from the surface becomes a critical factor for measuring the physical transport properties of quantum electronic materials. Consequently, the in-situ facility electronic transport measurements in vacuum condition and annealing temperature is a key factor while measuring the transport properties of quantum electronic materials.

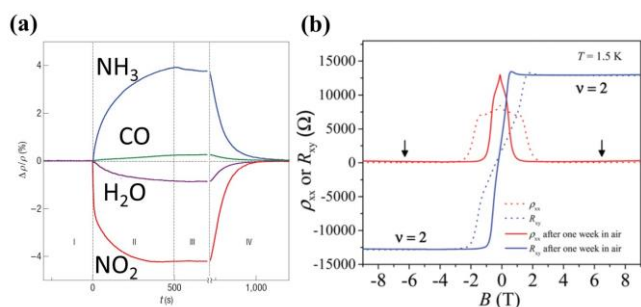


Fig. 1. (a) The resistance rate and exposing time of single-layer graphene by exposing different gases (NO_2 , H_2O , CO , NH_3) [11]; (b) the magnetoresistance in longitudinal and transverse resistance measurements of single-layer epitaxial graphene at 1.5 K. The dotted line represents the magnetoresistance measurements at the beginning, and the solid line represents the measurements after one week later after leaving the device in the air [12].

Dr. Chiashain Chuang when as a visiting scientist at the National Institute of Standards and Technology (NIST) in the United States encountered the problem of gas adsorption on the surface of single-layer epitaxial graphene, which affected the accuracy of quantum Hall resistance plateau in the Hall device of single-layer epitaxial graphene as shown in Fig. 1(b). This problem inspired him to innovate and improve in-situ electronic transport measurement methods on the low-temperature electronic transport fridge with a superconducting magnet, enabling him to measure longitudinal and transverse magnetoresistance in single-layer epitaxial graphene Hall devices with various carrier densities by vacuum annealing methods [12]. As shown in Fig. 2 (a), a typical low-temperature fridge system with a superconducting magnet requires a mechanical pump to evacuate the sample space to a vacuum of $P \sim 10^{-3}$ Torr. As a result, liquid helium can allow the sample to reach a minimum temperature of 1.5K and the magnetic field produced by the superconducting magnet can reach a maximum of 9 T. Dr. Chuang used his previous vacuum technique experiences and inspirations from handling silicon samples during his master's degree research experiences to grow clean ferromagnetic cobalt ultrathin films by annealing an Si (111) substrate in an ultra-high vacuum system ($P \sim 10^{-10}$ Torr) at 600 °C to desorb the adsorbed gases from air and organic pollutants from the silicon crystal surface [13]. By applying similar experiences to the low-temperature fridge system with a superconducting magnet system, we can isolate the single-layer epitaxial graphene

device in the vacuum chamber after closing the gate valve before lowering it into the sample space with a superconducting magnet as shown in Fig. 2 (a), and gradually heat it up from 323 K to 433 K, which is so called “vacuum annealing” methods after evacuating the chamber to $P = 10^{-3}$ Torr by using a mechanical pump. After keeping it at a fixed temperature for 5 minutes, the gate valve was opened and the sample was moved to the bottom sample space with a superconducting magnet for low-temperature magnetoresistance measurements under high magnetic fields. By repeating this vacuum annealing process, significant magnetoresistance changes can be observed as shown in Fig. 2 (b) [12]. It is found that the adsorption of gases from the atmosphere can significantly affect the carrier density of single-layer epitaxial graphene Hall devices. **In the case of electron-donor gases, such as NH_3 , the adsorbed molecules can introduce additional electrons to the graphene structure. This results in an increase in the carrier concentration as the excess electrons contribute to the overall electron population available for conduction. Conversely, electron-acceptor gases, like O_2 , can lead to a decrease in the carrier density by effectively removing electrons from the graphene lattice. It is important to note that the specific effect of gas adsorption on carrier concentration depends on the type of gas, its affinity for graphene, and the interaction mechanism involved [11].**

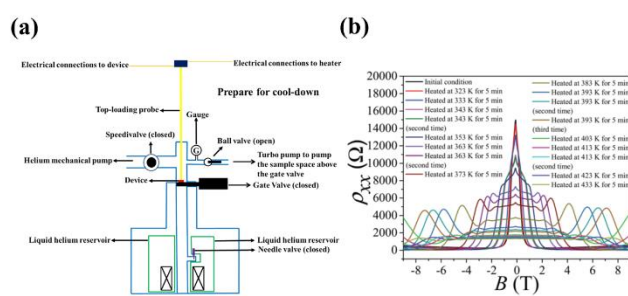


Fig. 2. (a) The schematic of the magnetoresistance measurement system using the He^4 cryogenic system at the NIST. (b) The variations in the longitudinal magnetoresistance of single-layer epitaxial graphene Hall device after 5 minutes of vacuum annealing at different temperatures [12].

Furthermore, we are able to leave the epitaxial graphene Hall device in the vacuum chamber above the closed gate valve and inject different kinds of gases into the chamber, allowing the graphene surface to absorb

one kind of gas overnight. After that, we can pump out the remaining gas and open the gate valve to insert the epitaxial Hall device into the sample space with a superconducting magnet for low-temperature magnetoresistance measurements. This experimental processes enable us to observe significant changes in longitudinal magnetoresistance as shown in Fig. 3 (a) and Hall magnetoresistance as shown in Fig. 3 (b) of the epitaxial graphene Hall device after being exposed to different kinds of gases [12]. Interestingly, we found that both water molecules and oxygen with positive charge from the air can gently induce a p-type doping effect for the epitaxial graphene to decrease the n-type carrier concentration of the epitaxial graphene, resulting in a distinct quantum Hall magnetoresistance plateau ($\nu = 2$) as shown in Fig. 3 (b) [12].

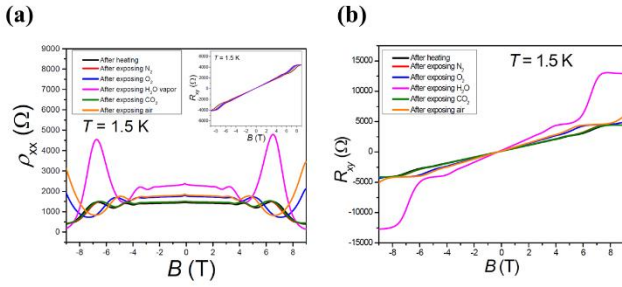


Fig. 3. (a) The longitudinal magnetoresistance of single-layer epitaxial graphene Hall device on different kinds of gases (N_2 , O_2 , H_2O , CO_2 and air) at $T = 1.5$ K after exposing the gases and the adsorption processes. The inset shows the Hall resistance. (b) The Hall resistance of single-layer epitaxial graphene Hall device on different kinds of gases (N_2 , O_2 , H_2O , CO_2 and air) [12].

On the other hand, the single-layer epitaxial graphene Hall device properties exhibit an interesting Hall magnetoresistance plateau ($\nu = 2$) at low temperature as a resistance standard. At room temperature ($T = 300$ K), the longitudinal resistivity ρ_{xx} reveals a nearly linear magnetoresistance transport behavior, which can be applied to the calibration of the magnetic field as shown in Fig. 4 (a). The inset shows the ρ_{xx} of different carrier densities at $T = 1.5$ K [14]. Furthermore, we also observed that the n-type epitaxial graphene could be converted to p-type in the atmosphere due to the absorption of enough water vapor and oxygen on the surface of epitaxial graphene. In that situation, we found that both p and n-type carrier densities are very low and show similar ρ_{xx} as shown in

Fig. 4 (b), which is near the Dirac point of graphene. Therefore, it could be applied to n-type and p-type mutual conversions in the future CMOS [15]. **Notably, the more pronounced effect induced by water vapor, as compared to oxygen, on the property of graphene can be attributed to the specific interaction mechanisms between these two gases and the graphene lattice. In the case of water vapor, it interacts with the graphene surface through adsorption and dissociation processes. When water vapor molecules are adsorbed onto the graphene, they dissociate into hydrogen (H) and hydroxyl (OH) radicals. The introduction of hydrogen and hydroxyl groups can alter the charge carrier concentration in the graphene layer. Therefore, the hydrogen atoms can effectively change the doping level and contribute to the observed dR_{xy}/dB slope change in electrical behavior due to Hall effect, leading to changes in longitudinal magnetoresistance and Hall resistance [11].**

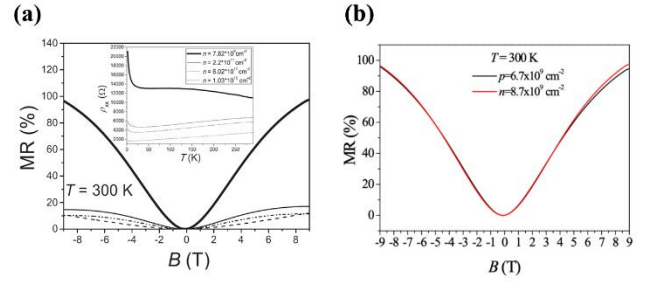


Fig. 4. (a) The ρ_{xx} of single-layer epitaxial graphene Hall device at room temperature ($T = 300$ K) with different carrier densities. The inset is the ρ_{xx} of different carrier densities at $T = 1.5$ K [14]. (b) At room temperature ($T = 300$ K), from p-type to n-type ρ_{xx} after gently vacuum annealing processes [15].

2. Experimental facilities and measurement results

Based on the above experimental experiences and techniques in vacuum annealing methods so as to change the transport properties of quantum electronic materials, we established a low-temperature closed cycle magnetoresistance measurement system (as shown in Fig. 5) in the Quantum Electronic Material Laboratory of the Department of Electronic Engineering, Chung Yuan Christian University (CYCU) [16]. The vacuum level of the measuring

system can be pumped to a high vacuum of 10^{-6} Torr (mechanical pump combined with turbo molecular pump), and the lowest temperature can be cooled down to 4.6 K and the highest temperature can be heated to 420 K. Furthermore, the maximum magnetic field can be reached to 1 Tesla. Therefore, using our unique measuring system vacuum annealing methods could be easily performed due to the upgrade of such a vacuum level, which could increase the efficiency of gas desorption and reduce the processing time of vacuum annealing processes. Our unique system could perform applied related research due to its high vacuum and low magnetic field range.

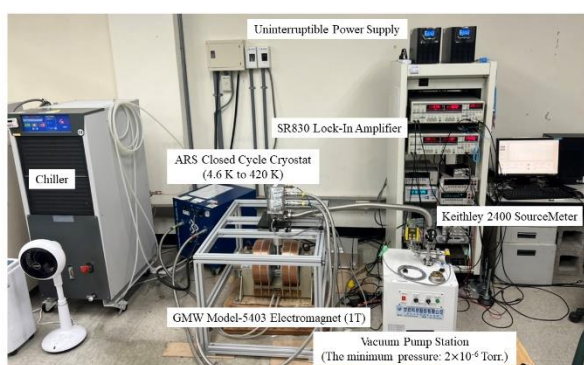


Fig. 5. The low-temperature closed cycle magnetoresistance measurement system of the Quantum Electronic Materials Laboratory in CYCU [16].

In order to perform the vacuum annealing processes in our low-temperature closed cycle magnetoresistance measuring system, we cooperated with Professor Dung-Sheng Tsai at the Department of Electronic Engineering in CYCU to study the magnetoresistance transport properties of nickel and copper-catalyzed graphene films by vacuum annealing [17]. Such films were prepared by the chemical vapor deposition technique. As shown in Fig. 6, in our measuring system we firstly decreased the sample temperature to 6 K as a stable measuring temperature to measure magnetoresistance under $P = 10^{-3}$ Torr before vacuum annealing. Then we pumped our system to 10^{-6} Torr and then increased the sample temperature to 375 K (around 102 °C, enough to desorb and pump out water vapor and oxygen) in one minute. Then we decreased the temperature to 6 K again and measured magnetoresistance after vacuum annealing. Fig. 6 (a) and (b) show that the magnetoresistance of nickel and copper-catalyzed graphene before and after vacuum annealing.

Obviously, the magnetoresistance significantly increased after vacuum annealing, which is consistent with the previous results about water vapor and oxygen from the air that can effectively compensate for the defects of graphene and neutralize excess charge impurities [12]. Figs. 6 (c) and (d) show magnetoresistance before and after vacuum annealing at low temperatures of 6 K and 15 K, respectively. Here the relative magnetoresistance is given by $MR_{\text{relative}} = [R_{\text{after}}(B) - R_{\text{before}}(B)] / R_{\text{before}}(B) \times (100\%)$, where $R_{\text{after}}(B)$ and $R_{\text{before}}(B)$ are the resistances at certain magnetic field before and after vacuum annealing, respectively. The percentage change of %resistance in our copper-catalyzed graphene is much higher than that in our nickel-catalyzed graphene, which indicates that nickel-catalyzed graphene quality is better due to less defects and charged impurities. Therefore, less water vapor and oxygen from the air could be adsorbed on the surface of the nickel-catalyzed graphene. Remarkably, nickel forms a stronger interaction with carbon due to the releasing carbon atoms to the nickel surface from nickel films, leading to a more controlled growth mechanism [18]. This results in fewer defects introduced during the initial stages of graphene formation. Copper, on the other hand, tends to exhibit a weaker interaction due to the carbon absorption on the copper surface, potentially leading to more defects and impurities [19].

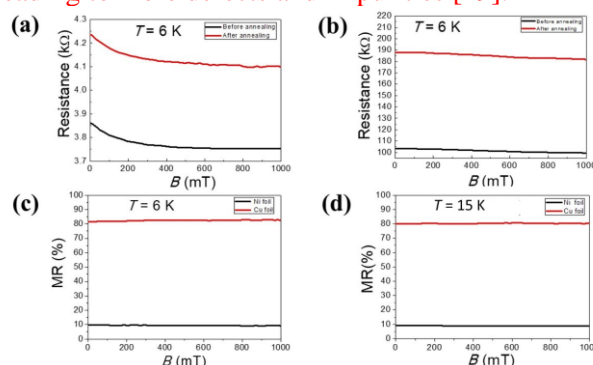


Fig. 6. Comparison of the magnetoresistance transport properties of nickel and copper-catalyzed graphene before and after vacuum annealing (a) the magnetoresistance of nickel-catalyzed graphene at $T = 6$ K before and after vacuum annealing (b) the magnetoresistance of copper-catalyzed graphene at $T = 6$ K before and after vacuum annealing (c) the relative magnetoresistance of nickel and copper-catalyzed graphene at $T = 6$ K after vacuum annealing in comparison with before vacuum annealing (d) the relative magnetoresistance of nickel and copper-catalyzed graphene at $T = 15$ K after vacuum annealing [17].

3. Conclusions and outlooks.

Vacuum annealing can effectively desorb the adsorbed gas on the surface of quantum electronic materials so as to affect their physical properties, such as electronic transport properties, magnetic properties, photoelectric properties and so on. We have tried to increase the vacuum level and heating temperature of our unique closed cycle measurement system, but we still need to pay attention to whether these vacuum annealing experimental steps would volatilize or damage our sample holder materials in our system. In future developments, we would try to inject a specific gas to observe its effects on our quantum electronic material samples.

We also cooperated with Professor Jyh-Shyang Wang from department of physics to grow Cd_3As_2 by molecular beam epitaxial method, Professor Yuan-Liang Zhong to grow MoS_2 by chemical vapor deposition method, and Professor Ya-Ping Hsieh from institute of atomic and molecular science, Academia Sinica to grow SnSe_2 also by chemical vapor deposition method to perform our vacuum annealing methods using our unique measuring system. It is found that the vacuum annealing process for the quantum electronic materials have a significant impact on their electronic transport properties. It is believed that this method could present a pertinent evaluation on the surface properties of novel 2D quantum materials that are expected to be used for quantum computations and chips.

Acknowledgments

This work was supported by the Ministry of Science and Technology (MOST), Taiwan (Grant nos. MOST 108-2112-M-033-001-MY3 and MOST 110-2112-M-033-009-MY3). One of the authors, Chiashain Chuang (CC), would like to thank Dr. Randolph E. Elmquist at National Institute of Standard and technology (NIST) for his useful discussions when CC worked at NIST.

References

1. K. S. Novoselov, A. K. Geim, S. V. Morozov, D. Jiang, Y. Zhang, S. V. Dubonos, I. V. Grigorieva and A. A. Firsov, *Science* **306**, 666 (2004).
2. A. Splendiani, L. Sun, Y. Zhang, T. Li, J. Kim, C.-Y. Chim, G. Galli and F. Wang, *Nano Lett.* **10**, 1271 (2010).
3. L. Li, Y. Yu, G. J. Ye, Q. Ge, X. Ou, H. Wu, D. Feng, X. H. Chen and Y. Zhang, *Nat. Nanotechnol.* **9**, 372 (2014).
4. K. Watanabe, T. Taniguchi and H. Kanda, *Nat. Mater.* **3**, 404 (2004).
5. X. Zhou, L. Gan, W. Tian, Q. Zhang, S. Jin, H. Li, Y. Bando, D. Golberg and T. Zhai, *Adv. Mater.* **27**, 8035 (2015).
6. Y.-Y. Wang, D.-R. Chen, J.-K. Wu, T.-H. Wang, C. Chuang, S.-Y. Huang, W.-P. Hsieh, M. Hofmann, Y.-H. Chang and Y.-P. Hsieh, *Nano Lett.* **21**, 6990 (2021).
7. W.-C. Chen, C. Chuang, T.-H. Wang, C.-C. Yeh, S.-Z. Chen, K. Sakanashi, M. Kida, L.-H. Lin, P.-H. Lee, P.-C. Wu, S.-W. Wang, K. Watanabe, T. Taniguchi, Y.-P. Hsieh, N. Aoki, C.-T. Liang, *2D Mater.* **9**, 045015 (2022).
8. S. Borisenko, Q. Gibson, D. Evtushinsky, V. Zabolotnyy, B. Büchner and R. J. Cava, *Phys. Rev. Lett.* **113**, 027603 (2014).
9. K.-L. Chiu, D. Qian, J. Qiu, W. Liu, D. Tan, V. Mosallanejad, S. Liu, Z. Zhang, Y. Zhao and D. Yu, *Nano Lett.* **20**, 8469 (2020).
10. Y. Guo, H. Deng, X. Sun, X. Li, J. Zhao, J. Wu, W. Chu, S. Zhang, H. Pan, X. Zheng, X. Wu, C. Jin, C. Wu and Y. Xie, *Adv. Mater.* **29**, 1700715 (2017).
11. F. Schedin, A. K. Geim, S. V. Morozov, E. W. Hill, P. Blake, M. I. Katsnelson and K. S. Novoselov, *Nat. Mater.* **6**, 652 (2007).
12. C. Chuang, Y. Yang, S. Pookpanratana, C. A. Hacker, C.-T. Liang and R. E. Elmquist, *Nanoscale* **9**, 11537 (2017).
13. C. Chuang, W. Y. Chang, W. H. Chen, J. S. Tsay, W. B. Su, H. W. Chang and Y. D. Yao, *Thin Solid Films* **519**, 8371 (2011).
14. C. Chuang, Y. Yang, R. E. Elmquist and C.-T. Liang, *Mater. Lett.* **174**, 118 (2016).
15. C. Chuang, C.-W. Liu, Y. Yang, W.-R. Syong, C.-T. Liang and R. E. Elmquist, *Materials* **12**, 2696 (2019).
16. J.-W. Ci, T.-W. Chiu, C.-Y. Liu, B.-X. Zeng, T.-Y. Fan, C.-W. Kuo, D.-S. Tsai, W.-Y. Uen, C. Chuang, *J. Taiwan Vacuum Society* **34**, 17 (2021).
17. B.-Y. Chen, P.-Y. Lai, B.-W. Chen, C.-Li Wu, M.-C. Li, Z.-Y. Fan, Y.-C. Wu, C.-L. Wu, C.-W. Kuo, H.-C. Wang, Y.-E. Chang, P.-H. Lee, D.-S. Tsai, C. Chuang, *Taiwan Vacuum Society* 2021.
18. A. Reina, X. Jia, J. Ho, D. Nezich, H. Son, V. Bulovic, M. S. Dresselhaus, J. Kong, *Nano Lett.* **9**, 30 (2009).
19. X. Li, W. Cai, J. An, S. Kim, J. Nah, D. Yang, R. Piner, A. Velamakanni, I. Jung, E. Tutuc, S. K. Banerjee, L. Colombo, R. S. Ruoff, *Science* **324**, 1312 (2009).